Published in final edited form as:
Nature. ; 485(7398): 381–385. doi:10.1038/nature11049.

Spatial partitioning of the regulatory landscape of the *X-inactivation center*

Elphège P. Nora[1], **Bryan R. Lajoie**[2,#], **Edda G. Schulz**[1,#], **Luca Giorgetti**[1,#], **Ikuhiro Okamoto**[1], **Nicolas Servant**[3], **Tristan Piolot**[1], **Nynke L. van Berkum**[2], **Johannes Meisig**[4], **John Sedat**[5], **Joost Gribnau**[6], **Emmanuel Barillot**[3], **Nils Blüthgen**[4], **Job Dekker**[2,*], and **Edith Heard**[1,*]

[1]Mammalian Developmental Epigenetics Group, Institut Curie, CNRS UMR 3215, INSERM U934, Paris 75248, France [2]Program in Gene Function and Expression, Department of Biochemistry and Molecular Pharmacology, University of Massachusetts Medical School, 01605-2324 Worcester, MA, USA [3]INSERM, U900, Paris F-75248 and Ecole des Mines ParisTech, Fontainebleau F-77300, France [4]Institute of Pathology, Charité–Universitätsmedizin and Institute of Theoretical Biology Humboldt Universität, Berlin, Germany [5]Department of Biochemistry and Biophysics, The Keck Center for Advanced Microscopy, University of California San Francisco, San Francisco, California, United States of America [6]Department of Reproduction and Development, Erasmus MC, University Medical Center, Rotterdam, The Netherlands

Summary

The mouse *X-inactivation center* (*Xic*) orchestrates initiation of X inactivation by controlling the expression of the non-coding Xist transcript. The full extent of *Xist's* regulatory landscape remains to be defined however. Here we use Chromosome Conformation Capture Carbon-Copy and super-resolution microscopy to analyse the spatial organisation of a 4.5Mb region including *Xist*. We uncover a series of discrete 200kb-1Mb topologically associating domains (TADs), present both before and after cell differentiation and on the active and inactive X. These domains align with several domain-wide epigenomic features as well as co-regulated gene clusters. Disruption of a TAD boundary causes ectopic chromosomal contacts and long-range transcriptional mis-regulation. *Xist*/*Tsix* illustrates the spatial segregation of oppositely regulated chromosomal neighborhoods, with their promoters lying in two adjacent TADs, each containing their known positive regulators. This led to the identification of a distal regulatory region of *Tsix* producing a novel long intervening RNA, Linx, within its TAD. In addition to uncovering a new principle of the *cis*-regulatory architecture of mammalian chromosomes, our study sets the stage for the full genetic dissection of the *Xic*.

*Correspondence: edith.heard@curie.fr, job.dekker@umassmed.edu.
#Equal contribution

Author information

High-throughput data are deposited in Gene Expression Omnibus under accession number GSE35721 for all 5C experiments and GSE34243 for microarray data. Correspondence should be addressed to EH (edith.heard@curie.fr) or JD (job.dekker@umassmed.edu).

Author contributions

EN, JD and EH designed the study and EN, EH and EGS wrote the manuscript with input from all authors, particularly LG. EN performed and analysed 3C, 5C, (RT-)qPCR, immunofluorescence, RNA and DNA FISH. BRL and NvB helped in the design and/or the analysis of 3C and 5C. LG performed 3C, FISH and 5C analysis. EGS generated the time-course transcriptomic data, which was analysed by JM and NB. IO performed FISH on pre-implantation embryos. JG donated the XTX mESC line. NS and EB helped in the epigenomic and 5C analyses. JS and TP set up OMX microscopy and analysis and TP performed structured illumination microscopy and image analysis.

In eukaryotes transcriptional regulation often involves multiple long-range elements and is influenced by the genomic environment[1]. A prime example of complex *cis*-regulation concerns the control of Xist expression by the *X-inactivation center* (*Xic*). The *Xic* has been defined by deletions and translocations as a region spanning several megabases[2,3]. However the extent of *Xic* sequences required for proper *Xist* regulation and X-chromosome inactivation (XCI) initiation remain unknown. Several elements in the vicinity of *Xist* are known to affect its activity, including the repressive antisense transcript Tsix and its regulators *Xite*, *DXPas34* and *Tsx*[4,5]. However, additional control elements must exist, as single-copy transgenes encompassing *Xist* and up to 460kb of flanking sequences are unable to recapitulate proper *Xist* regulation[6]. To characterise the *cis*-regulatory landscape of the *Xic* in an unbiased approach, we performed Chromosome Conformation Capture Carbon Copy (5C)[7] across a 4.5Mb region containing *Xist*.

We designed 5C-Forward and 5C-Reverse oligonucleotides following an alternating scheme[7], thereby simultaneously interrogating nearly 250,000 possible chromosomal contacts in parallel, with a mean resolution of 10–20 kb (Fig. 1a; see Methods). Analysis of undifferentiated mouse ES cells (mESCs) revealed that long-range (>50kb) contacts preferentially occur within a series of discrete genomic blocks, each covering 0.2–1Mb (Fig. 1b). These blocks differ from the higher-order organisation recently observed by Hi-C[8], corresponding to much larger domains of open or closed chromatin, that come together in the nucleus to form A and B-types of compartments[8]. Instead, our 5C analysis reveals self-associating chromosomal domains occurring at the sub-megabase scale. The size and location of these domains is identical in male and female mESCs (Supplementary Fig. 1) and in different mESC lines (Supplementary Fig. 2, Supplementary data 1).

We explored this organisation using 3D DNA FISH in male mESCs. Nuclear distances were significantly shorter between probes lying in the same 5C domain than in different domains (Fig 1c and d) and a strong correlation was found between 3D distances and 5C counts (Supplementary Fig. 3a and b). Furthermore, using pools of tiled BAC probes spanning up to 1Mb with structured illumination microscopy, we found that large DNA segments belonging to the same 5C domain colocalise to a greater extent than DNA segments located in adjacent domains (Fig. 1e), and this throughout the cell cycle (Supplementary Fig. 3c and d). Based on 5C and FISH data, we conclude that chromatin folding at the sub-megabase scale is not random, and partitions this chromosomal region into a succession of topologically associating domains (TADs).

We next investigated what might drive chromatin folding in TADs. We first noticed a striking alignment between TADs and the large blocks of H3K27me3 and H3K9me2[9] that are known to exist throughout the mammalian genomes[10,11,12,13] (e.g. TAD #E, Fig. 2 and Supplementary Fig. 4). We therefore examined 5C profiles of *G9a*$^{-/-}$ mESCs, which lack H3K9me2, notably at the *Xic*[14], and *Eed*$^{-/-}$ mESCs which lack H3K27me3[15]. No obvious change in overall chromatin conformation was observed, and TADs were not affected either in size or position in these mutants (Fig. 2, Supplementary Fig. 4b). Thus TAD formation is not due to domain-wide H3K27me3 or H3K9me2 enrichment. Instead, such segmental chromatin blocks might actually be delimited by the spatial partitioning of chromosomes into TADs.

We then addressed whether folding in TADS is driven by discrete boundary elements at their borders. 5C was performed in a mESC line carrying a 58kb deletion (ΔXTX[16]) encompassing the boundary between the *Xist* and *Tsix* TADs (#D and #E; Fig. 2b). We observed ectopic contacts between sequences in TADs #D and #E and an altered organisation of TAD #E. Boundary elements can thus mediate the spatial segregation of neighboring chromosomal segments. Within the TAD #D-#E boundary, a CTCF site was

recently implicated in insulating *Tsix* from remote regulatory influences[17]. However, alignment of CTCF and Cohesin binding sites in mESCs[18] with our 5C data revealed that although these factors are present at most TAD boundaries (Supplementary Fig. 4), they are also frequently present within TADs, excluding them as the sole determinants of TAD positioning. Furthermore, the fact that the two neighboring domains do not merge completely in ΔXTX cells (Fig. 2b) implies that additional elements, within TADs, can be usurped when a main boundary is removed. The factors underlying an element's capacity to act as a canonical or shadow boundary remain to be investigated.

Next we asked whether TAD organisation changes during differentiation or XCI. Both male neuronal progenitors (NPCs) and male primary mouse embryonic fibroblasts (MEFs) show similar organisation to mESCs, with no obvious change in TAD positioning. However, consistent differences in the internal contacts within TADs were observed (Fig.3a, Supplementary Fig. 2). Noticeably, some TADs were found to become lamina-associated domains (LADs)[19] at certain developmental stages (Fig. 3b). Thus chromosome segmentation into TADs reveals a modular framework where changes in chromatin structure or nuclear positioning can occur in a domain-wide fashion during development.

We then assessed TAD organisation on the inactive X (Xi), by first combining Xist RNA FISH, to identify the Xi, and super-resolution DNA FISH using BAC probe pools (as in Fig. 1e) on female MEFs. We found that colocalisation indices on the Xi were still higher for sequences belonging to the same TAD than to neighbouring TADs. The difference was however significantly lower for the Xi than for the Xa (Supplementary Fig. 5). Similarly, deconvolution of the respective contributions of the Xa and Xi from 5C data female MEFs (see methods, Supplementary Fig. 5) revealed that specific long-range contacts within TADs are lost on the Xi, but global TAD organisation remains, albeit it in a much attenuated form. This, together with a recent report focused on longer-range interactions[20], suggests that the Xi has a more random chromosomal organisation than its active homolog.

We next investigated how TAD organisation relates to gene expression dynamics during early differentiation. A transcriptome analysis, consisting of microarray measurements at 17 time points over the first 84 hours of female mESC differentiation was performed (Fig. 6a). During this time window, most genes in the 5C region were either up- or down-regulated. Statistical analysis demonstrated that expression profiles of genes with promoters located within the same TAD are correlated (Fig. 4b). This correlation is significantly higher than for genes in different domains (correlation coefficient of 0.03, $p<10^{-9}$) or for genes across the X chromosome in randomly selected, TAD-size regions (correlation coefficient of 0.09, $p<10^{-7}$). The observed correlations within TADs seems not to depend on distance between genes, and is thus distinct from previously described correlations between neighbouring genes[21] which decay on a length scale of ~100kb (Supplementary Fig. 6). Our findings suggest that physical clustering within TADs may be used to coordinate gene expression patterns during development. Furthermore, deletion of a boundary (ΔXTX) was accompanied by long-range transcriptional mis-regulation (Supplementary Fig.7), supporting a role for chromosome partitioning into TADs in long-range transcriptional control.

A more detailed analysis of each domain (Supplementary Fig. 6) revealed that co-expression is particularly pronounced in TADs #D #E and #F (Fig. 4b and c). Although correlations are strongest within TADs, there is some correlation between TADs showing the same trend, such as TADs #D and #F, which are both down-regulated during differentiation. Only TAD #E, which contains *Xist* and all of its known positive regulators (*Jpx, Ftx, Xpr, Rnf12*, supplementary Fig. 4d)[22] is anti-correlated with most other genes in the 4.5 Mb region, being up-regulated during differentiation (Supplementary Fig. 4c). The fact that these

coordinately up-regulated loci are located in the same TAD suggests that they are integrated into a similar *cis*-regulatory network, potentially sharing common *cis*-regulatory elements. We therefore predict that TAD #E (~550kb) represents the minimum 5′ regulatory region required for accurate Xist expression, explaining why even the largest transgenes tested so far (covering 150kb 5′ to *Xist*, Fig. 5) cannot recapitulate normal Xist expression[6].

The *Xist* and *Tsix* promoters lie in two neighbouring TADs with transcription crossing the intervening boundary (Fig. 2b), consistent with previous 3C experiments[22]. While the *Xist* promoter and its positive regulators are located in TAD#E, the promoter of its antisense repressor, *Tsix*, lies in TAD#D, which extends up to *Ppnx/Nap1L2,* >200kb away (Fig. 2b). Thus, in addition to the *Xite* enhancer, more distant elements within TAD #D may participate in *Tsix* regulation. To test this we used two different single-copy transgenic mouse lines, Tg53 and Tg80[23]. Both transgenes contain *Xist, Tsix* and *Xite* (Fig. 5a). Tg53 encompasses the whole of TAD #D, while Tg80 is truncated just 5′ to *Xite* (Fig. 5a; Supplementary Fig. 8). In the inner cell mass (ICM) of male E4.0 mouse embryos, Tsix transcripts could be readily detected from Tg53, as well as from the endogenous X (Fig. 5b). However, no Tsix expression could be detected from Tg80, which lacks the distal portion of TAD #D (Fig. 5b). Thus, sequences within TAD#D must contain essential elements for the correct developmental regulation of *Tsix*.

Within TAD#D, several significant chromosomal looping events involving the *Tsix* promoter and its enhancer *Xite* were detected (Fig. 2a and 5a, Supplementary Fig. 9). Alignment of 5C maps with enhancer signatures (Supplementary Fig. 8), suggested the existence of multiple regulatory elements within this region. We also identified a transcript initiating ~50kb upstream of the *Ppnx* promoter (Fig. 5a), from a region associated with pluripotency factor binding and corresponding to a predicted promoter for a large (80kb) intervening non-coding RNA (LincRNA[24], Supplementary Fig.9) which we termed Linx (Large INtervening transcript in the *Xic*). Linx RNA shares several features with ncRNAs, such as accumulation around its transcription site[25] (Fig. 5c), nuclear enrichment and abundance of the unspliced form[26] (Supplementary Fig.11 and 12). Linx and Tsix transcripts are co-expressed in the ICM of blastocysts from E3.5–4.0 onwards, as well as in male and female mESCs (Fig. 5c). Linx RNA is not detected earlier on in embryogenesis, nor in extra-embryonic lineages, implying an epiblast-specific function (Supplementary Fig. 8). Triple RNA FISH for Linx, Tsix and Xist in differentiating female mESCs (Supplementary Fig. 13) revealed that prior to Xist up-regulation, the probability of Tsix expression from alleles co-expressing Linx is significantly higher than from alleles that do not express Linx (Fig. 5d). Furthermore, Linx expression is frequently monoallelic, even prior to Xist up-regulation (Supplementary Figure 13), revealing a transcriptional asymmetry of the two *Xic* alleles prior to XCI. Taken together, our experiments based on 5C, transgenesis and RNA FISH, point towards a role for *Linx* in the long-range transcriptional regulation of *Tsix* – either through its chromosomal association with *Xite* and/or *via* the RNA it produces. This analysis of the *Xist/Tsix* region illustrates how the spatial compartmentalisation of chromosomal neighborhoods partitions the *Xic* into two large regulatory domains, with opposite transcriptional fates (Supplementary Fig. 12).

In conclusion, our study uncovers that sub-megabase folding of mammalian chromosomes results in the self-association of large chromosomal neighborhoods The stability of these TADs throughout differentiation, X-inactivation and in cell lines with impaired histone-modifying machineries suggests that this level of chromosome organisation may provide a basic framework onto which other domain-wide features, such as lamina association and blocks of histone modification, can be dynamically overlaid. Our data also point to a role for TADs in shaping regulatory landscapes, by defining the extent of sequences that belong to the same regulatory neighborhood. We anticipate that TADs may underlie previously

proposed regulatory domains based on functional and synteny conservation studies[27,28]. We believe that the principles we have revealed here will not be restricted to the *Xic*, as spatial partitioning of chromosomal neighborhoods occurs throughout the genome of mouse and human (see Dixon *et al.* in this issue of Nature), as well as *Drosophila*[29] and *E. coli*[30],. Future work will clarify the mechanisms driving this level of chromosomal organisation, and to what extent it generally contributes to transcriptional regulation. In summary, our study provides new insight into the *cis*-regulatory architecture of chromosomes that orchestrates transcriptional dynamics during development, and paves the way to dissecting the constellation of control elements of *Xist* and its regulators within the *Xic*.

Supplementary Material

Refer to Web version on PubMed Central for supplementary material.

Acknowledgments

We thank T. Pollex and T. Forné for experimental help; the imaging facility PICTIBiSA@BDD for technical assistance, D. Gentien and C. Hego from the Institut Curie for microarray hybridisations. We thank K. Bernhard, F. Stewart and A. Smith, who in the context of the EU FP7 SYBOSS (Grant No. 242129) provided protocols and material for 2i culture and EpiSC differentiation. We are grateful to members of EH laboratory for critical input. This work was funded by grants from the Ministère de la Recherche et de l'Enseignement Supérieur and the ARC (to EN); a HFSP Long term fellowship (LT000597/2010-L) (to EGS). EU EpiGeneSys FP7 Network of Excellence no. 257082, the Fondation pour la Recherche Medicale, ANR and ERC Advanced Investigator award no. 250367 (to EH). N.B. was supported by BMBF (FORSYS) and EMBO (fellowship ASTF 307-2011). JD, BRL and NvB were supported by NIH (R01 HG003143) and a W.M. Keck Foundation Distinguished Young Scholar Award.

References

1. Kleinjan DA, Lettice LA. Long-range gene control and genetic disease. Advances in Genetics. 2008; 61:339–388. [PubMed: 18282513]
2. Rastan S. Non-random X-chromosome inactivation in mouse X-autosome translocation embryos--location of the inactivation centre. J Embryol Exp Morphol. 1983; 78:1–22. [PubMed: 6198418]
3. Rastan S, Robertson EJ. X-chromosome deletions in embryo-derived (EK) cell lines associated with lack of X-chromosome inactivation. J Embryol Exp Morphol. 1985; 90:379–388. [PubMed: 3834036]
4. Augui S, Nora EP, Heard E. Regulation of X-chromosome inactivation by the X-inactivation centre. Nat Rev Genet. 2011; 12:429–442. [PubMed: 21587299]
5. Anguera MC, et al. Tsx Produces a Long Noncoding RNA and Has General Functions in the Germline, Stem Cells, and Brain. PLoS Genet. 2011; 7:e1002248. [PubMed: 21912526]
6. Heard E, Mongelard F, Arnaud D, Avner P. Xist yeast artificial chromosome transgenes function as X-inactivation centers only in multicopy arrays and not as single copies. Molecular and cellular biology. 1999; 19:3156. [PubMed: 10082582]
7. Dostie J, et al. Chromosome Conformation Capture Carbon Copy (5C): A massively parallel solution for mapping interactions between genomic elements. Genome Research. 2006; 16:1299–1309. [PubMed: 16954542]
8. Lieberman-Aiden E, et al. Comprehensive Mapping of Long-Range Interactions Reveals Folding Principles of the Human Genome. Science. 2009; 326:289–293. [PubMed: 19815776]
9. Marks H, et al. High-resolution analysis of epigenetic changes associated with X inactivation. Genome Research. 2009; 19:1361–1373. [PubMed: 19581487]
10. Pauler FM, et al. H3K27me3 forms BLOCs over silent genes and intergenic regions and specifies a histone banding pattern on a mouse autosomal chromosome. Genome Research. 2009; 19:221–233. [PubMed: 19047520]
11. Wen B, Wu H, Shinkai Y, Irizarry RA, Feinberg AP. Large histone H3 lysine 9 dimethylated chromatin blocks distinguish differentiated from embryonic stem cells. Nat Genet. 2009; 41:246–250. [PubMed: 19151716]

12. Lienert F, et al. Genomic Prevalence of Heterochromatic H3K9me2 and Transcription Do Not Discriminate Pluripotent from Terminally Differentiated Cells. PLoS Genet. 2011; 7:e1002090. [PubMed: 21655081]
13. Hawkins RD, et al. Distinct epigenomic landscapes of pluripotent and lineage-committed human cells. Cell Stem Cell. 2010; 6:479–491. [PubMed: 20452322]
14. Rougeulle C, et al. Differential histone H3 Lys-9 and Lys-27 methylation profiles on the X chromosome. Molecular and cellular biology. 2004; 24:5475. [PubMed: 15169908]
15. Montgomery ND, et al. The murine polycomb group protein Eed is required for global histone H3 lysine-27 methylation. Curr Biol. 2005; 15:942–947. [PubMed: 15916951]
16. Monkhorst K, Jonkers I, Rentmeester E, Grosveld F, Gribnau J. X Inactivation Counting and Choice Is a Stochastic Process: Evidence for Involvement of an X-Linked Activator. Cell. 2008; 132:410–421. [PubMed: 18267073]
17. Spencer RJ, et al. A Boundary Element Between Tsix and Xist Binds the Chromatin Insulator Ctcf and Contributes to Initiation of X Chromosome Inactivation. Genetics. 201110.1534/genetics.111.132662
18. Kagey MH, et al. Mediator and cohesin connect gene expression and chromatin architecture. Nature. 2010; 467:430–435. [PubMed: 20720539]
19. Peric-Hupkes D, et al. Molecular Maps of the Reorganization of Genome-Nuclear Lamina Interactions during Differentiation. Molecular Cell. 2010; 38:603–613. [PubMed: 20513434]
20. Splinter E, et al. The inactive X chromosome adopts a unique three-dimensional conformation that is dependent on Xist RNA. Genes & Development. 201110.1101/gad.633311
21. Caron H, et al. The Human Transcriptome Map: Clustering of Highly Expressed Genes in Chromosomal Domains. Science. 2001; 291:1289–1292. [PubMed: 11181992]
22. Tsai CL, Rowntree RK, Cohen DE, Lee JT. Higher order chromatin structure at the X-inactivation center via looping DNA. Developmental Biology. 2008; 319:416–425. [PubMed: 18501343]
23. Heard E, et al. Transgenic mice carrying an Xist-containing YAC. Human molecular genetics. 1996; 5:441. [PubMed: 8845836]
24. Guttman M, et al. Chromatin signature reveals over a thousand highly conserved large non-coding RNAs in mammals. Nature. 2009; 458:223–227. [PubMed: 19182780]
25. Khalil AM, et al. Many human large intergenic noncoding RNAs associate with chromatin-modifying complexes and affect gene expression. Proceedings of the National Academy of Sciences. 2009; 106:11667.
26. Seidl CIM, Stricker SH, Barlow DP. The imprinted Air ncRNA is an atypical RNAPII transcript that evades splicing and escapes nuclear export. EMBO J. 2006; 25:3565–3575. [PubMed: 16874305]
27. Ruf S, et al. Large-scale analysis of the regulatory architecture of the mouse genome with a transposon-associated sensor. Nat Genet. 2011; 43:379–386. [PubMed: 21423180]
28. Kikuta H, et al. Genomic regulatory blocks encompass multiple neighboring genes and maintain conserved synteny in vertebrates. Genome Research. 2007; 17:545–555. [PubMed: 17387144]
29. Sexton T, et al. Three-Dimensional Folding and Functional Organization Principles of the Drosophila Genome. Cell. 2012; 148:458–472. [PubMed: 22265598]
30. Mercier R, et al. The MatP/matS Site-Specific System Organizes the Terminus Region of the E. coli Chromosome into a Macrodomain. Cell. 2008; 135:475–485. [PubMed: 18984159]

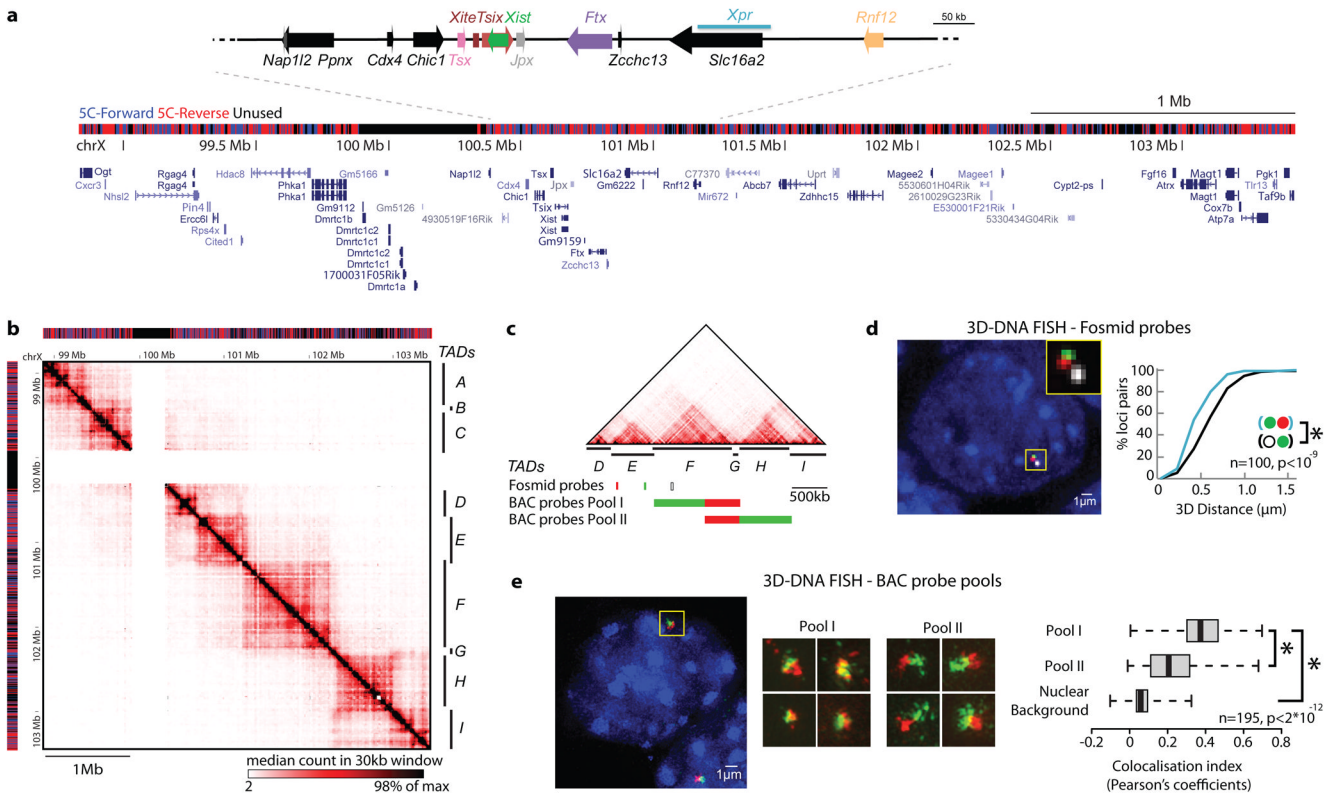

Figure 1. Chromosome partitioning into topologically assocating domains (TADs)

a, Distribution of 5C-Forward and 5C-Reverse HindIII restriction fragments across the 4.5 Mb analysed showing positions of RefSeq Genes and known XCI regulatory loci. **b,** 5C datasets from XY undifferentiated mESCs (E14), displaying median counts in 30kb windows every 6kb. Chromosomal contacts are organised into discrete genomic blocks (TADs A-F). A region containing segmental duplications excluded from the 5C analysis is masked (white). **c,** Positions of DNA FISH probes. **d,** Interphase nuclear distances are smaller for probes in the same 5C domain. **e,** Structured illumination microscopy reveals that colocalisation of neighbouring sequences is greater when they belong to the same 5C domain. Boxplots display the distribution of Pearson correlation coefficient between red and green channels, with whiskers and boxes encompassing all and 50% of values respectively; central bars denote the median correlation coefficient. Statistical significance was assessed using Wilcoxon's rank-sum test.

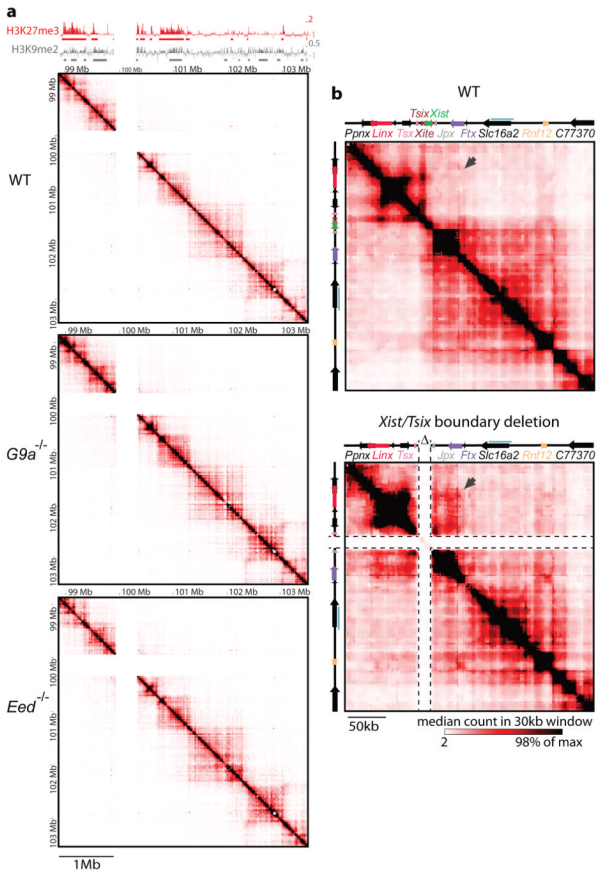

Figure 2. Determinants of topologically associating domains

a, Blocks of contiguous enrichment in H3K27me3 or H3K9me2[11] align with the position of TADs (Chip-chip from[9]) but TADs are largely unaffected in the absence of H3K9me2 in male *G9a*$^{-/-}$ cells or H3K27me3 or in male *Eed*$^{-/-}$ cells. **b**, Deletion of a boundary at *Xist/Tsix* disrupts folding pattern of the two neighboring TADs.

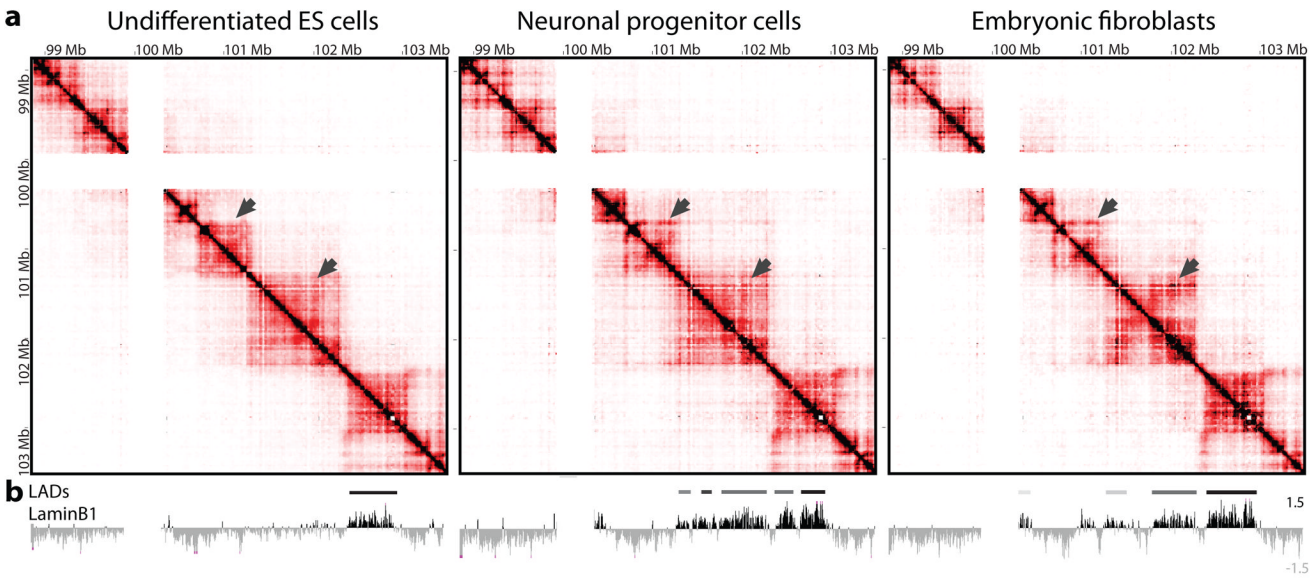

Figure 3. Dynamics of topologically associating domains during cell differentiation

a. Comparison of 5C data from male mESCs (E14), NPCs (E14) and primary MEFs reveals general conservation of TAD positions during differentiation, but differences in their internal organisation (arrows highlight examples of tissue-specific patterns). **b** Lamina associated domains (LADs, from ref.[19]) align with TADs. Chromosomal positions of tissue-specific LADs reflect gain of lamina association by TADs, as well as internal reorganisation of lamina associated TADs during differentiation.

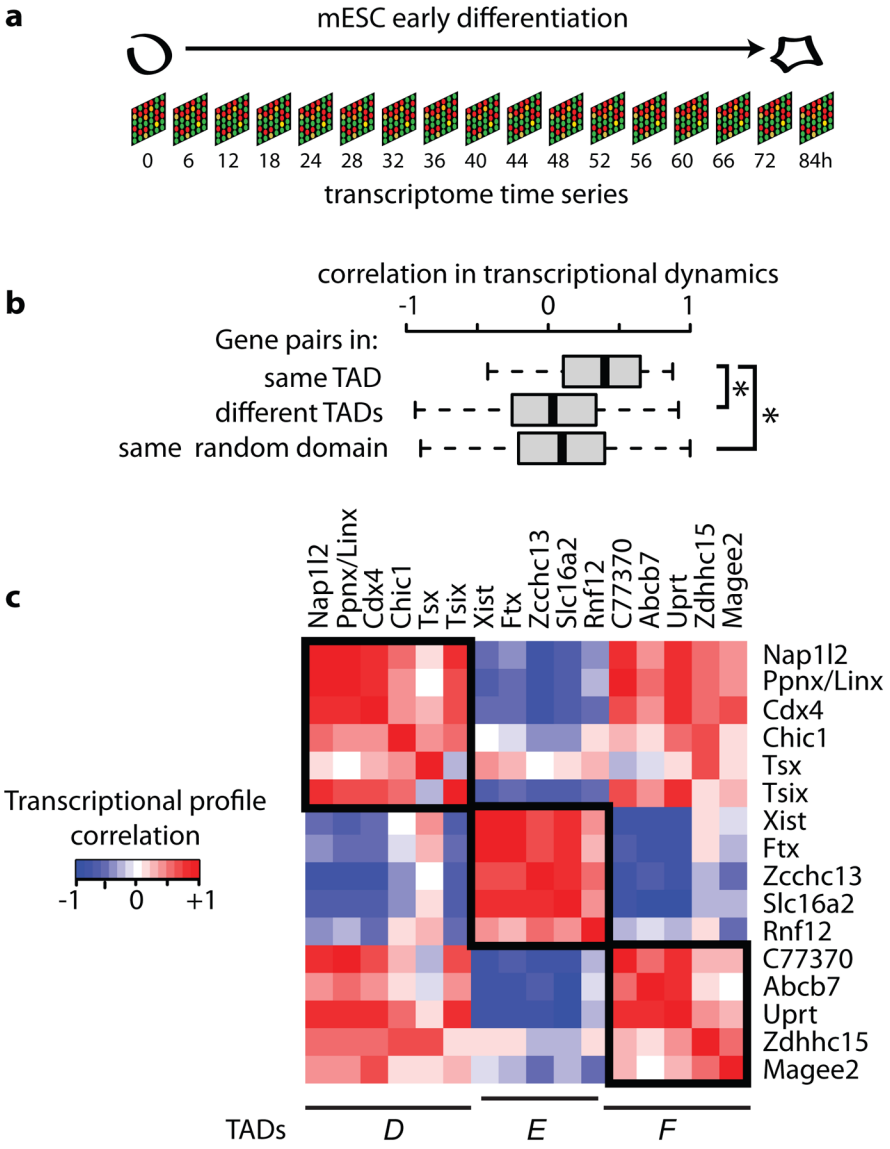

Figure 4. Transcriptional co-regulation within topologically associating domains

a, Female mESCs were differentiated towards epiblast stem cell lineage for 84 hours. Transcript levels were measured every 4–6 hours at 17 different time points by mircoarray analysis. **b,** Pearson's correlation 15 coefficients over all time points were calculated for (1) gene pairs lying in the same TAD, (2) pairs in different TADs and (3) for pairs in randomly defined domains on the X-chromosome that contain a similar number of genes and are of comparable size. Box plots display the distribution of Pearson's correlation coefficients, with whiskers and boxes encompassing all and 50% of values respectively, and central bars denoting the median correlation coefficient. * represents significant difference with $p<10^{-7}$ using Wilcoxon's ranksum test. **c,** Pearson's correlation coefficients for gene pairs in TADs #D, #E and #F with red denoting positive and blue negative correlation. Boxes indicate the TAD boundaries.

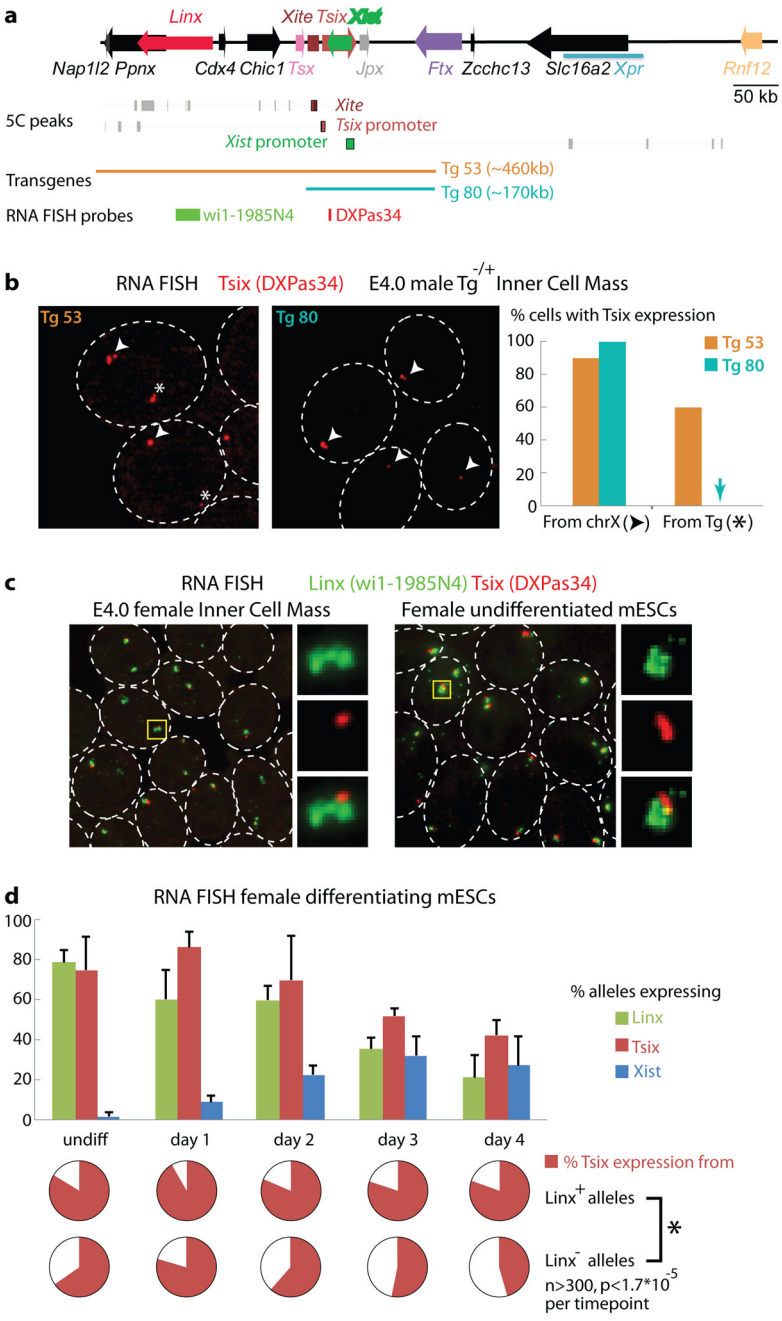

Figure 5. 5C maps reveal new regulatory regions in the *Xic*

(a) 5C maps at the restriction fragment resolutions (male E14 mESCs) show that *Tsix* and *Xist* promoters belong to two distinct neighbouring TADs, respectively spanning >200kb and >550kb (male E14 mESCs). **b,** Corresponding statistically significant looping events (5C peaks) for restriction fragments within *Xite*, *Tsix* promoter or *Xist* promoter within their respective TAD. The Tg80 YAC transgene lacks genomic elements found to interact physically with *Xite/Tsix* that are present in Tg53. **c,** RNA FISH analysis of Tsix Tsix expression is detected in the inner cell masses of heterozygous transgenic male E4.0 embryos by RNA FISH from single-copy paternally inherited Tg53 but not Tg80 transgenes. Transgenic (star) and endogenous *Tsix* alleles (arrowhead) were discriminated by

subsequent DNA FISH as in supplementary Fig. 5. n=20 ICM cells (2 embryos each). **d**, Linx transcripts (green, wi1–1985N4 probe) are expressed in both E4.0 ICM cells and mESCs, together with Tsix (red, DXPas34 probe), and unspliced transcripts accumulate locally in a characteristic cloud-like shape. **e,** RNA FISH in differentiating female mESCs revealing synchronous downregulation of Linx and Tsix with concomitant up-regulation of Xist (detected with a strand-specific probe). Barrs are the standard deviation around the mean of three experiments. **f**, Triple-color RNA FISH allowing simultaneous detection of Linx, Tsix and Xist RNAs. Scoring of Xist-negative alleles demonstrates that prior to Xist up-regulation Tsix expression is more frequent from Linx-expressing alleles than from Linx non-expressing alleles, at all time-points tested. Presented is the mean of three experiments. Statistical differences were assessed using Fisher's exact test. Cells were differentiated in monolayers by LIF withdrawal.